Hairpin-Line and Hybrid Hairpin-Line/Half-Wave Parallel-Coupled-Line Filters

EDWARD G. CRISTAL AND SIDNEY FRANKEL

Abstract—**A new class of microwave filters, hairpin-line and hybrid hairpin-line/half-wave parallel-coupled-line filters, is reported. This class of filters is particularly well suited for microstrip and TEM printed-circuit realizations because grounding of the filter resonators is generally not required. Hairpin-line filters have been divided into two types. The first (Type A) is characterized by having its input and output lines open-circuited at their ends. The Type A filter has been found to yield practical impedance levels for narrow to approximately 25-percent bandwidths. The second (Type B) is characterized by having its input and output lines short-circuited at their ends. However, because of space limitations, details of the Type B filter are not presented in this paper. Theoretical background and design equations for Type A bandpass filters are presented. Experimental data for several stripline filters of 5- and 20-percent bandwidths are given. Experimental results for two microwave-integrated-circuit (MIC) filters are discussed.**

I. Introduction

THE USE of stripline and/or microwave-integrated-circuit (MIC) designs in microwave systems is often preferred to other manufacturing methods because of advantages with respect to size, weight, costs, and usually reproducibility. MIC is particularly useful in hybrid integrated circuits. Circuits and systems constructed in stripline or MIC would preferably utilize geometries not requiring connections to ground, since realization of such connections is awkward in most cases. Among the numerous transmission-line filter designs available, the half-wave parallel-coupled-line filter satisfies the above condition. Hairpin-line filters also satisfy the above condition, although, to date, theory and design equations for these filters have been unavailable. The purposes of the present paper are 1) to present an approximate design theory for hairpin-line filters that is satisfactory for filter bandwidths of very narrow to approximately 20 to 25 percent; 2) to present filter design equations; and 3) to present experimental data for several hairpin-line and hybrid hairpin-line/half-wave parallel-coupled-line filters.

The image impedance and propagation constant for the infinite periodic hairpin line have been previously reported [1]. Equivalent circuits for several periodically terminated lines, including the Type A hairpin line, were discussed at the IEEE Region 6 Conference [2]. However, for finite-length hairpin-line filters, neither exact nor approximate design equations have been reported.

Manuscript received November 8, 1971; revised June 8, 1972. This work was conducted at the Stanford Research Institute, Menlo Park, Calif. 94025, and supported principally by the U. S. Army Electronics Command Laboratories under Contract DAAB07-70-C-0044. The revised paper was financially supported by the National Research Council of Canada under Grant A8242.

E. G. Cristal was with the Stanford Research Institute, Menlo Park, Calif. 94025. He is now with the Department of Electrical Engineering and the Communications Research Laboratory, McMaster University, Hamilton, Ont., Canada.

S. Frankel is at P.O. Box 126, Menlo Park, Calif. 94025.

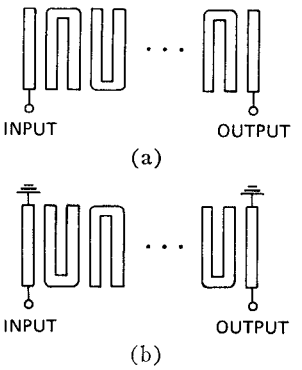

Fig. 1. Hairpin-line filters. (a) Type A. (b) Type B.

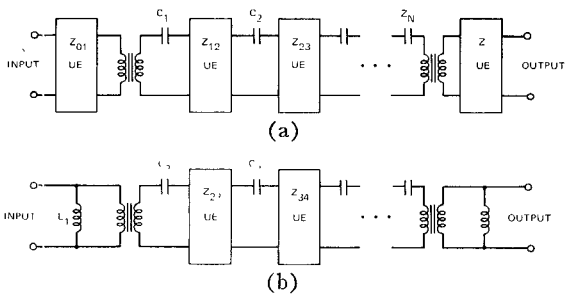

Fig. 2. Equivalent circuits for hairpin-line filters. C_i represents the open-circuited transmission line of characteristic impedance C_i. L_i represents the short-circuited transmission line of characteristic impedance L_i. UE represents the unit element of characteristic impedance $Z_{i,i+1}$. (a) Equivalent circuit for hairpin-line filter of Fig. 1(a). (b) Equivalent circuit for hairpin-line filter of Fig. 1(b)

The Type A and B hairpin-line filters are shown schematically in Fig. 1(a) and (b), respectively. Equivalent circuits for the filters of Fig. 1 have been derived by the authors and are presented in Fig. 2(a) and (b), respectively. These circuits are based on the assumption that *inductive* coupling beyond the nearest neighbors is negligible (i.e., a sparse inductance-matrix assumption). For commonly used microwave-filter geometries using parallel-coupled-line arrays, this assumption differs from, and is more difficult to satisfy, than the usual one of negligible capacitive coupling beyond the nearest neighbors (i.e., a sparse capacitance-matrix assumption). Physically, the difference can be understood in terms of the basic definitions of the coupling parameters. In the case of the admittance (capacitance) parameters,

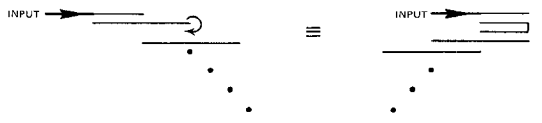

Fig. 3. Folding procedure for obtaining a hairpin-line filter from a half-wave parallel-coupled-line filter.

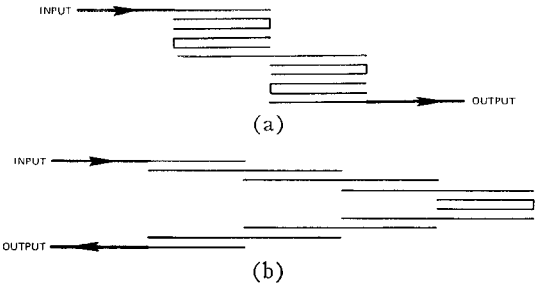

Fig. 4. Examples of hybrid hairpin-line/half-wave parallel-coupled-line filters.

the nearest neighbors act as partial electric shields between a conductor and the next-nearest neighbor. In the impedance-parameter (inductive) case, the "floating" conductors only slightly effect the tendency of magnetic field lines to spread out over the entire coupled array.

The reason for making the former rather than the latter assumption is the enormous simplification that results in the equivalent circuits for the Type A and B hairpin-line filters. The assumption of negligible capacitive coupling beyond the nearest neighbors leads to very complex equivalent circuits that preclude any likelihood of achieving practical design procedures. Ultimately, since approximations are necessary in either approach, the practicality of either assumption must be judged on the basis of comparisons between theoretical and experimental results. Nevertheless, several examples are presented that compare computed filter responses based on both sparse-inductance and sparse-capacitance matrix assumptions, so that the reader may judge from a theoretical viewpoint at what point and to what extent the approximate design method becomes unsatisfactory.

Conceptually, hairpin-line filters may be obtained by folding the resonators of parallel-coupled half-wave open-circuited resonator filters. Fig. 3 illustrates the process. The first half-wave resonator is folded into a hairpin, giving the hybrid hairpin-line/half-wave parallel-coupled-line filter shown on the right. Next, if desired, the second half-wave line may be folded, giving a second hairpin and a new hybrid filter. The process may be continued as many times as the designer wishes. Clearly, a large number of hybrid physical realizations is possible. It has been determined that the coupling between turns introduced by the folding process must be accounted for in designs having couplings greater than approximately 24 dB. However, in all cases the same design equations presented herein may be used, and same basic electrical performance results. Fig. 4(a) and (b) illustrates two hybrid filters. The filter of Fig. 4(a) consists of one half-wave and four hairpin resonators, while the filter of Fig. 4(b) consists of one hairpin and six half-wave resonators.

Three of the principal advantages of the approximate design equations and theory presented herein are as follows. 1) In the limiting case (half-wave parallel-coupled-line filters), the equations are identical with those previously published [5]. 2) The theory allows the designer to go from all hairpin-line to hybrid hairpin-line/half-wave parallel-coupled-line to all half-wave parallel-coupled-line designs in a straightforward and simple manner. 3) The coupling between pairs of lines constituting hairpin resonators may be chosen arbitrarily and may be individually adjusted at any point in the design.

In the following discussions and design equations, the parameter cp is used to denote the coupling in decibels between line pairs constituting hairpin resonators. This parameter is used initially in a qualitative sense in order to judge the relative degree of "coupling" (and consequently closeness of spacing) between line pairs constituting hairpin resonators. A value of $cp = \infty$ corresponds to no coupling. In other words, the corresponding line pair has degenerated into a linear half-wave resonator. A precise mathematical definition for cp will be given in Section III.

In Section II, theoretical and experimental results are presented and discussed for trial Type A filters constructed in both stripline and MIC. Design procedures and equations are given in Section III. In Section IV a summary and conclusions are stated.

II. Theoretical and Experimental Results

A. Theory

In order to theoretically check the range of validity of the approximate design equations and equivalent circuit given in Fig. 2(a) and [2], a number of filters having bandwidths of from 5 to 20 percent were designed using the procedures in Section III. The responses of these filters were first calculated using the equivalent circuit of Fig. 2(a) and then recalculated using a more accurate (but very complex) equivalent circuit derived by the graph transformation method of Sato–Cristal [3]. The latter equivalent circuit is based on a sparse-capacitance-matrix assumption, and therefore should give computed results closer to experiment. A few typical responses are presented and discussed below.

The VSWR responses for a four-resonator hairpin-line filter, having a nominal fractional bandwidth of $w = 0.05$ and theoretical passband ripple of 1.355, are shown in Fig. 5 for three values of hairpin resonator coupling (cp value in decibels). The theoretical response computed using the equivalent circuit of Fig. 2(a) is depicted by the solid line for any value of cp. This response is identical to the one that would be obtained for half-wave parallel-coupled-line filters using the design equations of Cristal [5]. Also, the equivalent circuit of Fig. 2(a) and that obtained by the graph transformation method [3] are identical for $cp = \infty$. Theoretical responses based on the more accurate equivalent circuit

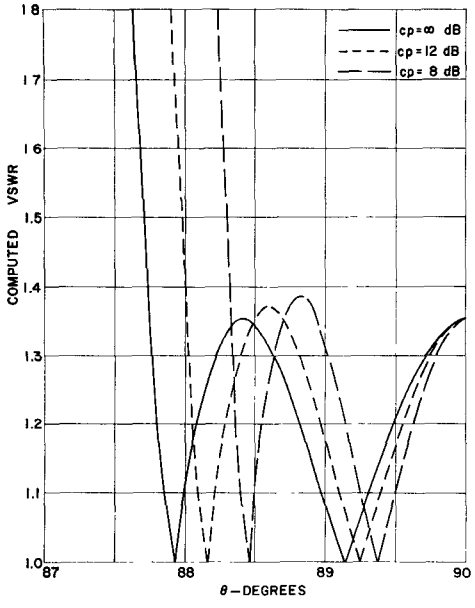

Fig. 5. Computed VSWR responses using approximate and exact equivalent circuits ($N=4$, $w=0.05$).

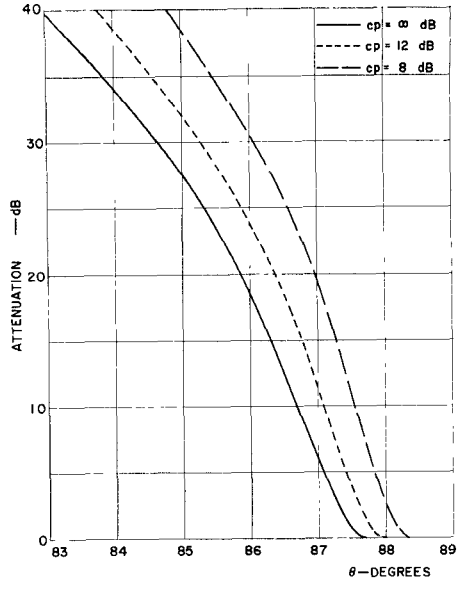

Fig. 6. Computed selectivity responses using approximate and exact equivalent circuits ($N=4$, $w=0.05$).

for cp = 8 and 12 dB are depicted by the long-dash and short-dash curves, respectively. Note that the more accurate analysis predicts a bandwidth contraction that is a function of cp, which becomes larger as cp decreases (tighter coupling). However, in all cases the VSWR response remains nearly equiripple. It should be pointed out that for stripline and MIC planar geometries, 8-dB coupling is near the limit of practical realization. Thus the curve for cp = 8 dB is essentially a worst case. In practice, cp values of from 10 to 20 dB would usually be selected, so that typical responses would lie approximately in the range between the cp = 12 and the infinite-decibel curve.

Fig. 6 presents the corresponding selectivity curves. As expected, the differences in the curves merely reflect the effects of the diminished bandwidths for the tighter coupled cases.

Figs. 5 and 6 represent typical results for narrow-bandwidth filters. Fig. 7 presents calculated VSWR responses for 4 resonator hairpin-line filters having design bandwidths of $w=0.15$, theoretical passband VSWR's of 1.355, and cp values of 12 and ∞ dB. (A third curve denoted as "Curve *A*" is also shown. This curve will be discussed later.) Again, the more accurate analysis reveals a bandwidth contraction from the nominal value. But, again the VSWR is nearly equiripple over the diminished bandwidth.

In all of the cases examined in the above manner, the bandwidth calculated using the more accurate equivalent circuit was less than the nominal value and was a function of the cp value. Surprisingly, however, the *percentage bandwidth contraction* was found to be virtually independent of the nominal design bandwidth and N, the number of filter resonators. Consequently, it is possible to plot the relative bandwidth contraction as a function of cp in a single universal curve. This has been done in Fig. 8, which was computed for 0.01- and 0.10-

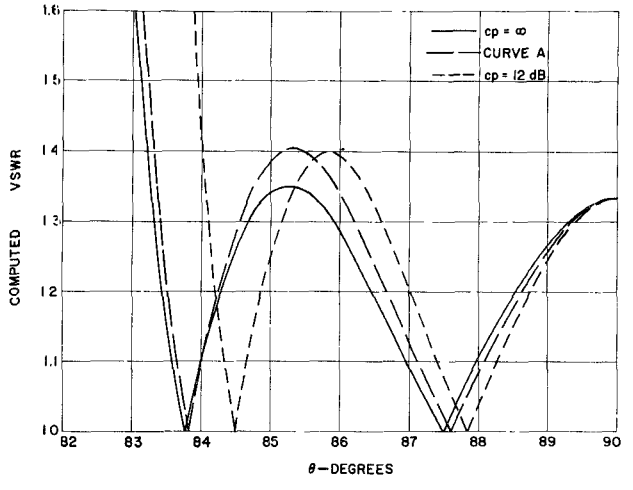

Fig. 7. Computed VSWR responses using approximate and exact equivalent circuits ($N=4$, $w=0.15$).

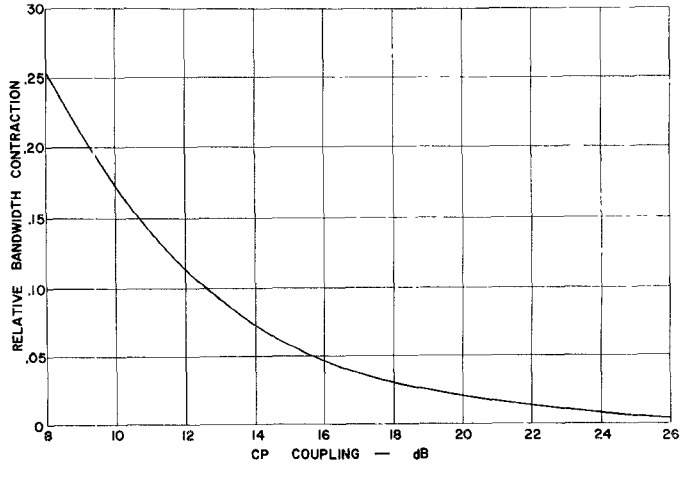

Fig. 8. Relative bandwidth contraction versus coupling parameter cp.

TABLE I
SUMMARY OF EXPERIMENTAL FILTER SPECIFICATIONS

	Filter Type	Fractional Bandwidth	Resonators	Passband Ripple (dB)	Media	Dielectric	Ground Plane Spacing or Substrate Thickness and Roughness
1	Hairpin-line	0.05	4	0.1	stripline	Tellite, $\epsilon_r = 2.32$	$b = 0.250$ in
2	Hybrid	0.05	4	0.1	stripline	Tellite, $\epsilon_r = 2.32$	$b = 0.250$ in
3	Hairpin-line	0.20	5	0.1	stripline	Rexolite, $\epsilon_r = 2.54$	$b = 0.250$ in
4	Hairpin-line	0.05	4	0.1	MIC	99.6-percent alumina, $\epsilon_r = 9.7$	$h = 0.025$ in 10 μ-in
5	Hairpin-line	0.20	7	0.1	MIC	99.6-percent alumina, $\epsilon_r = 9.7$	$h = 0.025$ in 10 μ-in

dB ripple filters for $N = 4$ through 11 resonators. In all cases, deviations from the plotted curve were less than 0.5 percent. The curve may be utilized in two ways: 1) to analyze a hairpin-line filter using the simplified equivalent circuit of Fig. 2(a) by first multiplying the nominal bandwidth by 1—the ordinate value from Fig. 8, and 2) to design a hairpin-line filter to have a specified fractional bandwidth w by first dividing the nominal value by 1—the ordinate value from Fig. 8, and then substituting the result into the design equations given in Section III.

A result of the latter technique is illustrated by Curve A in Fig. 7. In this case, in order to achieve a 0.15 fractional bandwidth filter with cp = 12 dB, a design value of

$$w \approx \frac{0.15}{1 - 0.112} = 0.168$$

was used in the design equations in Section III. The resulting VSWR (Curve A) is seen to be quite satisfactory.

B. Experiment

In order to experimentally check the range of validity of the theory and filter design equations, a number of trial stripline and MIC Type A filters were constructed with widely differing bandwidths. The nominal electrical and material specifications for several of the experimental filters are summarized in Table I. Some comments on the experimental results follow.

1) Stripline Filters: Filters 1, 2, and 3 were constructed in stripline, with 0.25-in ground plane spacing. Filter 1 was a hairpin-line filter of the type depicted in Fig. 1(a). Its nominal design bandwidth and center frequency were 5 percent and 1.5 GHz. The measured attenuation and return loss are shown in Fig. 9. The midband attenuation is approximately 2.5 dB. The bandwidths measured between points of 10-dB and 12-dB return loss are approximately 0.044 and 0.035, respectively. This filter was designed with a cp value of 12 dB. Using the contraction data of Fig. 8, the anticipated bandwidth is

$$w \approx 0.05 \times (1 - 0.112) = 0.044.$$

The experimentally determined bandwidth is seen to be smaller. It is believed that the additional bandwidth contraction results from the finite length connections between line pairs constituting hairpin resonators that are not accounted for in the theory. In practice, this could be compensated for by increasing the coupling slightly between the interior resonators of the filter.

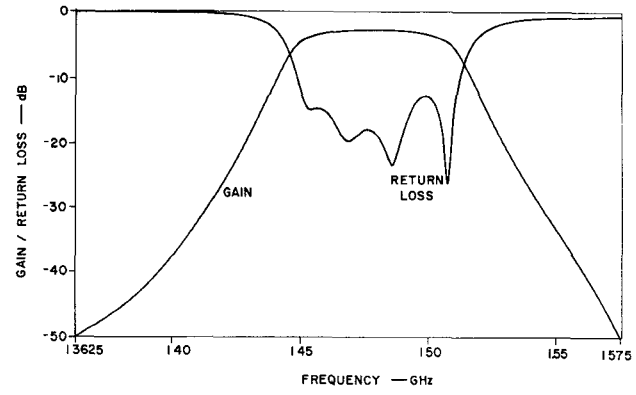

Fig. 9. Measured attenuation and return loss for trial stripline filter 1.

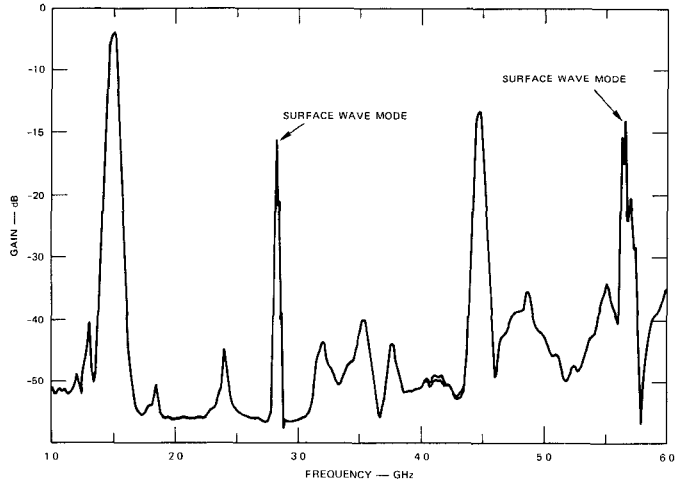

Fig. 10. Measured wide-band frequency response of stripline hairpin-line filter 1.

A wide-band swept frequency response for filter 1, shown in Fig. 10, shows numerous low-level spurious responses, typically 40 dB down or more, which were caused by plane-wave modes excited by tuning screws. However, additionally there is a noticeable spurious response at 2.8 GHz that has been identified as a surface-wave mode. This mode was nearly always excited in the experimental hairpin-line filters. However, its magni-

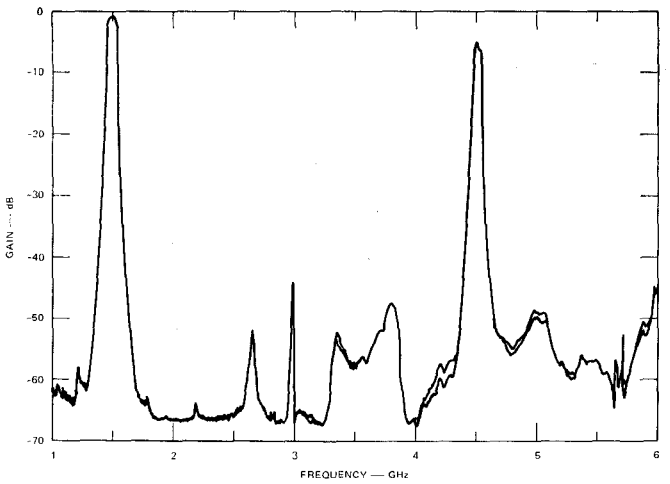

Fig. 11. Measured wide-band frequency response of hybrid stripline filter 2.

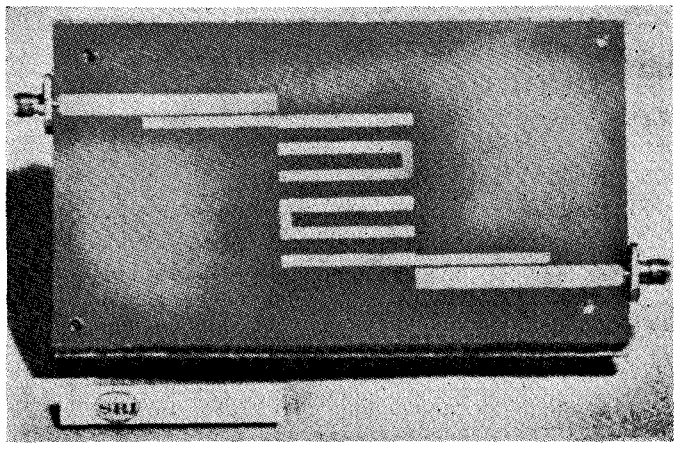

Fig. 12. Hybrid hairpin-line/half-wave parallel-coupled-line filter 2.

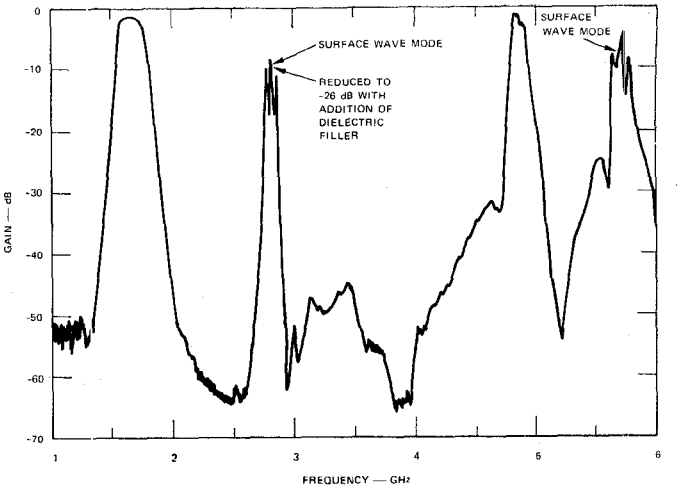

Fig. 13. Measured wide-band frequency response of stripline hairpin-line filter 3.

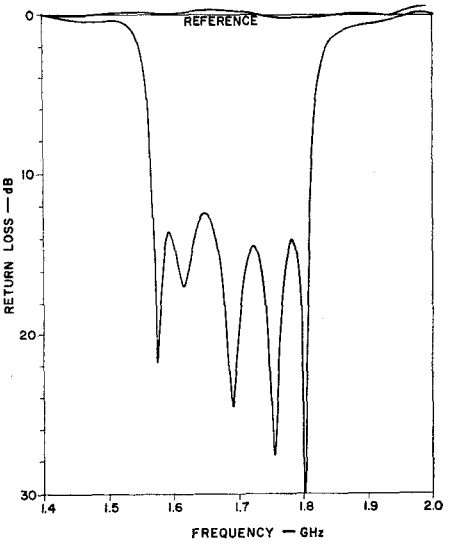

Fig. 14. Measured return loss for trial stripline filter 3.

tude could be substantially reduced in two ways: 1) by using hybrid hairpin-line/half-wave parallel-coupled-line geometries, or 2) by using a dielectric filler to eliminate air gaps between the dielectric interface. The result of the first technique is illustrated by the measured response shown in Fig. 11. Fig. 11 gives the attenuation data for filter 2, which had identical electrical specifications as filter 1, but was constructed in a hybrid hairpin-line/half-wave parallel-coupled-line configuration. A photograph of filter 2 is shown in Fig. 12. The reason that this method greatly reduces the spurious response at $2f_0$ is that the hybrid geometry interrupts the path of the surface-wave mode, while at the same time the TEM mode does not couple at $2f_0$. Note that the spurious mode was reduced by approximately 25 dB in this case.

Results of the second method are illustrated by the data given in Fig. 13. These data are for the hairpin-line filter 3, whose design was of 5 resonators and 20-percent bandwidth. The second method attempts to eliminate or reduce the coupling to the surface-wave mode by eliminating air gaps between the dielectric interfaces. Fig. 13 shows that without a dielectric filler (but with the ground planes tightly clamped together), there was a narrow spurious passband at $\approx 2f_0$, which was only about 10 dB down. However, insertion of a dielectric filler (Vaseline petroleum jelly, $\epsilon_r \approx 2.5$) reduced the spurious response to about -26 dB.

Fig. 14 presents the measured return loss in the passband for filter 3. The measured fractional bandwidth between points of 12-dB and 14-dB return loss are 0.144 and 0.135, respectively. The cp value for this filter was 8 dB, so that the expected fractional bandwidth would be

$$w \approx 0.20 \times (1 - 0.255) = 0.149.$$

The measured bandwidth is again smaller than the "theoretical," which is consistent with the previous results for the narrower bandwidth filters.

2) MIC Filters: In order to experimentally evaluate the design theory and equations with regard to MIC filters, filters 4 and 5 of Table I were constructed and tested. Photographs of these filters are shown in Fig.

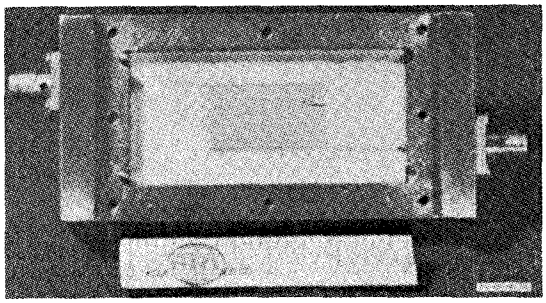

(a)

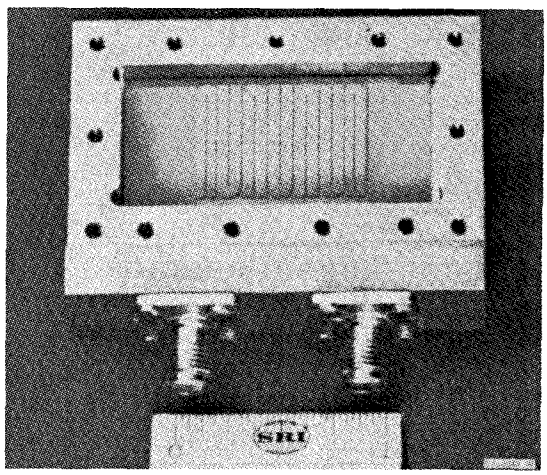

(b)

Fig. 15. MIC hairpin-line trial filters. (a) Filter 4. (b) Filter 5.

15(a) and (b), respectively. In order to avoid possible difficulties that might have been encountered because of differing even- and odd-mode velocities, a metal cover plate was placed 0.025 in above the alumina substrates. This compensated the velocities and resulted in an effective dielectric constant of $\epsilon_r = 5.35$ for the media.[1] The measured attenuation response in the vicinity of the passband for filter 4 corresponded moderately well with theoretically computed data. The measured VSWR showed only two points of match, indicating that the filter was not optimally tuned. However, the peak VSWR was within the specifications (1.36 or less) so that further tuning was not pursued. The bandwidth measured between frequencies of 1.35 VSWR (0.1-dB ripple) was 4.5 percent, which corresponded reasonably well with the value that would be obtained using the contraction factor from Fig. 8. In practice, a small adjustment in the resonator couplings would have brought this up to specification. The attenuation and VSWR responses in the vicinity of the passband for filter 5 showed the same qualitative behavior as that of filter 4.

A serious discrepancy between the theory and experimental results for MIC filters was the appearance of significant wide-band spurious responses in the stopband of the filters. These were determined to be due to a surface-wave mode that was briefly mentioned in the discussion of stripline filters. The surface-wave mode was always strongly excited in MIC media. The cutoff frequency for this mode corresponds (approximately) to when the hairpin resonators are a wave length *in the dielectric*. In stripline filters, the surface-wave mode propagates at $f \approx 2f_0$, where f_0 is the center frequency of the filter. However, the MIC media the surface-wave mode propagates are considerably less than $2f_0$. For MIC filters on alumina ($\epsilon_r = 9.7$), the surface-wave cutoff frequency is only slightly greater than f_0. Consequently, the stopband attenuation response is badly degraded. Suppression of the surface-wave mode in MIC can only be accomplished with hybrid geometries.

III. Design Procedures

A. Hairpin-Line-Filter Equations

The equivalent circuit for the Type A hairpin-line filter, shown in Fig. 2(a), is topologically dual to the well-known interdigital filter. Hence, the existing design tables and approximate design procedures may be utilized after suitable modifications for hairpin-line filter designs. Space does not allow for the detailed development of the design equations; however, the essential design procedures are summarized below. We first present approximate design equations that were developed by modifying those given in [5].

First to be defined is the set of prototype filter parameters and auxiliary equations given in Table II. N is the order of the low-pass prototype filter, having a cutoff frequency of ω_1' and normalized element values g_i. Tables of g_i values are available that give Chebyshev, Butterworth, and other types of responses [6], [7]. The parameter cp in Table II is the coupling between line pairs constituting a single hairpin resonator, and not between adjacent hairpin resonators. Mathematically, cp has been defined as[2]

$$\text{cp} = -10 \log_{10} \frac{L_{ij}}{\sqrt{L_{ii}L_{jj}}}, \qquad \text{for } j = i + 1 \qquad (1)$$

where the L_{ij} parameters are defined in (2). Once the cp factor is chosen, the *initial* synthesized design will consist of hairpin resonators all having the same cp value. However, a simple method is presented later for obtaining arbitrary and different values of cp for each resonator, if desired.

A hairpin-line filter based on an N-order low-pass prototype filter will consist of $2N+2$ parallel-coupled lines. The array of $2N+2$ coupled lines is completely defined in terms of its inductance matrix which, for the assumed coupling conditions, can be written as

[1] An alternate method would have been to use "wiggly lines" as described by Podell [4].

[2] The equation for cp was originally $\text{cp} = -20 \log_{10} (L_{ij}/\sqrt{L_{ii}L_{jj}})$, which is more logical than (1). However, the computer software was mistakingly written using (1), and all of the experimental and most of the theoretical data were compiled before the error was noticed.

TABLE II

AUXILIARY EQUATIONS AND PARAMETER DEFINITIONS

N order of low-pass prototype filter;

g_i low-pass prototype filter element values ($i = 0, 1, 2, \cdots, N+1$);

ω_1' low-pass prototype radian cutoff frequency;

w fractional bandwidth of the microwave filter;

$w = 2\dfrac{f_2 - f_1}{f_2 + f_1} = \dfrac{f_2 - f_1}{f_0}$, where f_1 and f_2 are the lower and upper band-edge frequencies of the microwave filter and f_0 is the bandcenter;

$\theta_1 = \dfrac{\pi}{2}\left(1 - \dfrac{w}{2}\right)$;

$\tau = \dfrac{1}{2}\tan\theta_1$;

$G_i = \dfrac{1}{\sqrt{\omega_1' g_{i-1} g_i}}$, for $i = 1$ and $N+1$;

$G_i = \dfrac{1}{\omega_1' \sqrt{g_{i-1} g_i}}$, for $i = 2, 3, \cdots, N$;

cp hairpin coupling in decibels;

$k = 10^{-|\mathrm{cp}/10|}$

h arbitrary positive dimensionless parameter usually less than 1 which controls the immittance level in the filter interior.

For $i = 1$ and $N+1$	For $i = 2, 3, \cdots, N$
$A_{11}^{(i)} = 1$	$A_{11}^{(i)} = h\tau$
$A_{12}^{(i)} = \sqrt{h}\, G_i$	$A_{12}^{(i)} = hG_i \sin\theta_1$
$A_{22}^{(i)} = h[G_i^2 + \tau]$	

TABLE III

DESIGN EQUATIONS FOR HAIRPIN-LINE FILTERS

$L_{pp} = \dfrac{A_{22}^{(i)} + A_{11}^{(i+1)}}{2(1-k)}$ $L_{p+1,p+1} = L_{pp}$	$p = 2i$ $i = 1, 2, \cdots, N$
$L_{11} = A_{11}^{(1)}$	
$L_{2l+2,2N+2} = A_{11}^{(N+1)}$	
$L_{p,p+1} = A_{12}^{(i)}$	$p = 2i - 1$ $i = 1, 2, \cdots, (N+1)$
$L_{p,p+1} = kL_{pp}$	$p = 2i$ $i = 1, 2, \cdots, N$

where

v velocity of propagation in the medium;

L_{ij} $l_{ij}/(Z_A v^{-1})$;

l_{ij} self- or mutual inductance per unit length of the ith and jth conductors;

Z_A source impedance.

In terms of the auxiliary equations given in Table II, the L_{ij} are given by Table III. Having obtained the normalized inductance matrix from Table III, the normalized capacitance matrix may be computed by the formula

$$[C] = [L]^{-1} \tag{3}$$

where

C_{ij} $c_{ij}/(v^{-1} Y_A)$;

c_{ij} self- or mutual capacitance per unit length of the ith and jth conductors;

Y_A $1/Z_A$.

The normalized parameters C_{ij} may be converted into the convenient form c_{ij}/ϵ by the equation

$$c_{ij}/\epsilon = \frac{376.7}{\sqrt{\epsilon_r}}\, Y_A C_{ij} \tag{4}$$

where

ϵ_r effective relative dielectric constant of the medium;

ϵ $\epsilon_0 \epsilon_r$;

ϵ_0 permittivity of free space.

From the numerical values for c_{ij}/ϵ, the physical dimensions of the coupled lines may be determined from various design charts.

If the L matrix is sparse, as is the case here, the C

$$\text{inductance matrix normalized to } Z_A v^{-1} = \begin{bmatrix} L_{11} & L_{12} & 0 & 0 & \cdots & 0 \\ L_{12} & L_{22} & L_{23} & & & \\ 0 & L_{23} & L_{33} & L_{34} & 0 & \cdots 0 \\ \cdot & & L_{34} & L_{44} & L_{45} & \\ \cdot & & & \cdot & & \\ \cdot & & & & \cdot & \\ \cdot & & & & & L_{2N+2,2N+2} \end{bmatrix} \tag{2}$$

matrix will generally be dense. (It may even represent a nonphysical system.) However, only the diagonal and the upper and lower subdiagonal entries are of significance.[3] Other entries will generally be small in comparison, at least for narrow-band filters, and may be neglected. However, as the filter bandwidth is increased, the nonprincipal terms of the C matrix will also increase. Since it is known that the capacitance matrix is approximately sparse for the planar-array filter configurations ordinarily used at microwave frequencies, checking the nonprincipal terms is one way of estimating when the filter responses may begin to deviate appreciably from the theoretically expected behavior.

As noted previously, the equations in Table III give designs consisting of hairpin-line resonators, all of which have the same cp value. However, we present next a simple transformation that allows modification of the

[3] These will be referred to as principal terms or principal entries. All other entries will be referred to as nonprincipal.

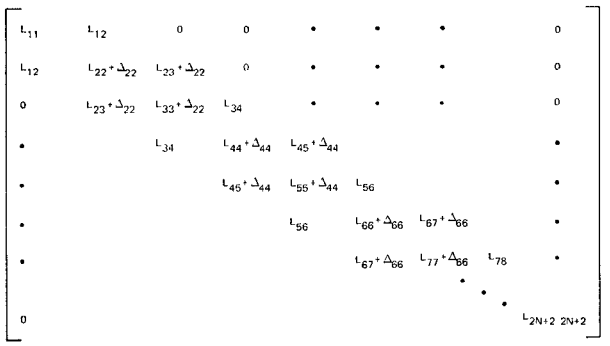

Fig. 16. Matrix transformation that leaves hairpin-line filter responses invariant.

TABLE IV
NORMALIZED L-VALUES FOR EXAMPLE HYBRID FILTER OF FIG. 12

Normalized L-Matrix		
I	$L(I, I)$	$L(I, I+1)$
1	1.00000	0.30031
2	1.40641	0.08874
3	1.40641	0.08303
4	1.35828	0.08570
5	1.35828	0.06571
6	1.35828	0.08570
7	1.35828	0.08303
8	1.40641	0.08874
9	1.40641	0.30031
10	1.00000	
Normalized L-Matrix		
I	$L(I, I)$	$L(I, I+1)$
1	1.00000	0.30031
2	1.31767	0.00000
3	1.31767	0.08303
4	1.35828	0.08570
5	1.35828	0.06571
6	1.35828	0.08570
7	1.35828	0.08303
8	1.31767	0.00000
9	1.31767	0.30031
10	1.00000	

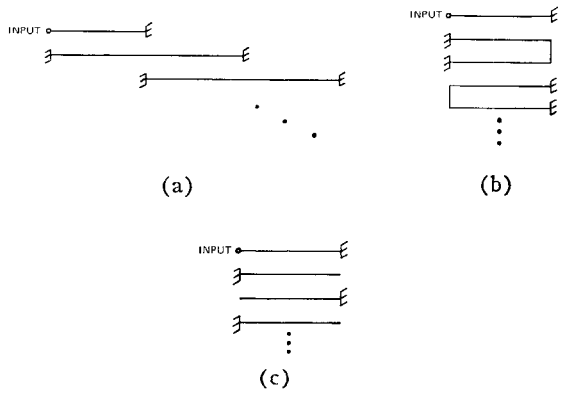

Fig. 17. Progressive steps in transforming a parallel-coupled-line filter into an interdigital filter. (a) Parallel-coupled line filter. (b) Intermediate wicket form for interdigital filter. (c) Final form for interdigital filter.

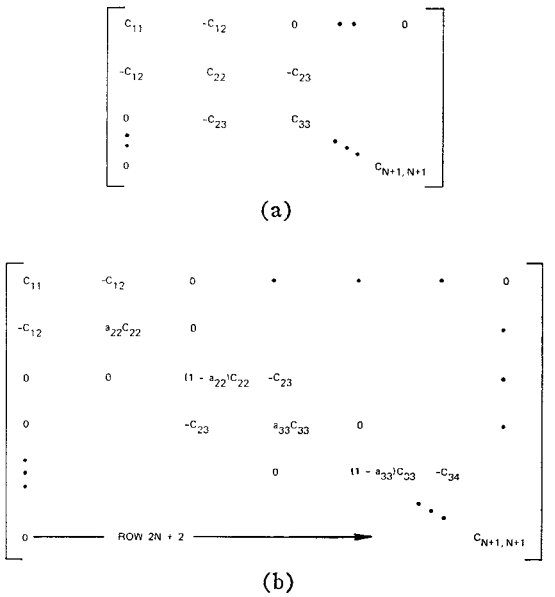

Fig. 18. Capacitance matrices for equivalent interdigital and wicket filters. (a) Interdigital filter capacitance matrix. (b) Wicket filter capacitance matrix.

coupling between two lines forming a hairpin, and by which hybrid hairpin-line/half-wave parallel-coupled-line filters may be designed.

B. Design of Hybrid Hairpin-Line/Half-Wave Parallel-Coupled-Line Filters

The detailed theory for hairpin-line filters of the type under discussion reveals that their responses are invariant, provided that the expression

$$L_{ii} - 2L_{i,i+1} + L_{i+1,i+1}, \qquad \text{for } i = 2, 4, 6, \cdots, (2N) \quad (5)$$

remains constant. In addition, physical realizability requires

$$L_{ii} - L_{i,i-1} - L_{i,i+1} > 0, \qquad \text{for all } i. \quad (6)$$

The L_{ij} parameters in (5) correspond to the self- and mutual inductance between line pairs constituting hairpin resonators. Thus it is evident that there is considerable redundancy and flexibility in determining suitable numerical values for the hairpin resonators.

A matrix transformation that satisfies (5), is easily programmed on a computer, and whose effect on the filter geometry is easily visualized, is depicted in Fig. 16. Note that the even-numbered rows have the increment Δ_{ii} added to the appropriate L_{ij} values in a way that satisfies (5). Thus all values Δ_{ii} not violating (6) give physically realizable inductance matrices corresponding to equivalent hairpin-line filters.

The transformation

$$\Delta_{ii} = -L_{i,i+1}, \qquad i = 2, 4, \cdots, (2N) \quad (7)$$

is particularly useful, for in this case no inductive (and no capacitive) coupling exists between lines originally constituting a hairpin resonator. *In other words,* (7) *transforms the hairpin resonator into a half-wave parallel-coupled-line resonator.* Repeated application of (7) per-

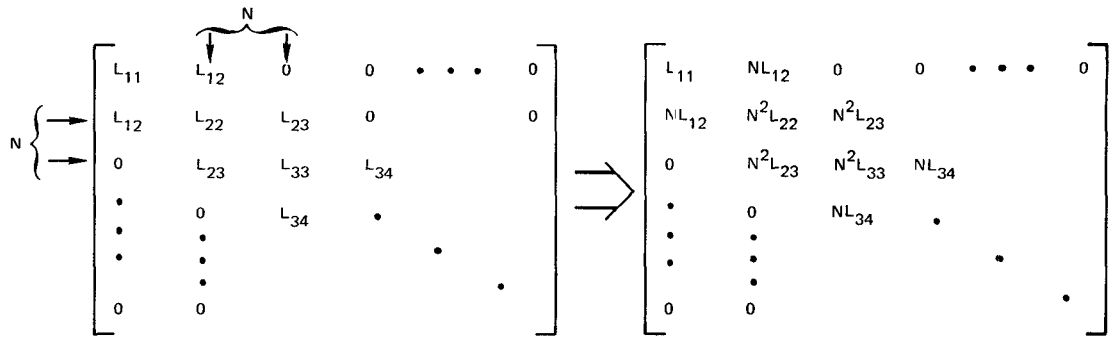

Fig. 19. Example of inductance transformation for hairpin-line filters.

mits the design of hybrid hairpin-line/half-wave parallel-coupled-line structures. The following example will serve as an illustration. The original L-matrix for the filter shown in Fig. 12 with a hairpin-resonator coupling of 12 dB (cp = 12 dB) is given in the upper half of Table IV. The physical realization of the filter for this matrix would be an all-hairpin-line filter like that in Fig. 1(a). By letting

$$\Delta_{88} = \Delta_{22} = -0.08874 \tag{8}$$

the results given in the lower half of Table IV are obtained. This leads to the physical configuration of Fig. 12.

C. Designs Using Exact Tables

The use of the preceding transformation allows in a straightforward way the application of exact design tables for interdigital filters [8] to the design of hybrid hairpin-line/half-wave parallel-coupled-line filters. In order to present the method concisely we summarize below some needed facts concerning the design of interdigital filters. The reader is referred to [6], [9] for additional details on interdigital filters. The interdigital filter may be conceptualized as the result of folding the half-wave parallel-coupled-line filter shown in Fig. 17(a) into the intermediate "wicket filter" shown in Fig. 17(b). Then, since the grounded ends of the wickets are physically close and at the same potential, they may be connected, yielding the interdigital form given in Fig. 17(c). The original justification for this folding procedure was based on physical considerations [9]. The folding process has since been verified mathematically [3]. The wicket filter and the hairpin-line filter are electrical duals. Consequently, if the interdigital filter in Fig. 17(c) can be converted back to the wicket form in Fig. 17(b), the principle of duality may be applied to achieve a hairpin-line filter design.

It is well known that the capacitance matrix given in Fig. 18(a) can uniquely represent an interdigital filter of the form shown in Fig. 17(c). Tables of c_{ij} are available that yield optimum Chebyshev and maximally flat responses [8]. Space does not permit, but it can be proved that the $(N+1)\times(N+1)$ capacitance matrix shown in Fig. 18(a) corresponding to an interdigital filter can be expanded into the $(2N+2)\times(2N+2)$ matrix shown in Fig. 18(b), with the latter corresponding to a wicket filter in which there is no coupling between any line pair constituting a wicket. Furthermore, the responses of the wicket and interdigital filters will be identical. The parameters a_{ii} in Fig. 18(b) are real, but at this intermediate point need not satisfy any other conditions. Of course, if the wicket filter itself were to be realized, then each row of the capacitance matrix of Fig. 18(b) would have to satisfy (6) with L replaced by C.

At this point it is perhaps evident how to proceed. The C_{ij} of Fig. 18(b) are to be replaced by L_{ij} (with suitable normalization), so that the matrix formally represents a half-wave parallel-coupled-line filter with open-circuited resonators. Next, the transformations depicted in Fig. 16 are performed to obtain the particular hybrid hairpin-line/parallel-coupled-line filter desired. The L-matrix is then inverted to obtain the C-matrix, which is then physically realized.

D. Inductance-Matrix Transformations

A second transformation that is useful is a special form of inductance congruence transformation that is very similar to capacitance-matrix transformations [10]. The effect of this transformation is to scale the impedance level at specific points within the filter, without changing its transfer response. The transformation as applied to the *interior sections* of the filter is illustrated in Fig. 19. Note that the transformation must be performed on *paired rows and paired columns*, in distinction to conventional capacitance-matrix transformations. The allowed pairs of rows and columns are

$$\text{row–columns } i \text{ and } i+1, \qquad \text{for } i = 2, 4, \cdots, 2N. \tag{9}$$

The only exceptions to this rule are when transforming the input and output impedances. In order to modify these or, equivalently, to change the terminations, row–column 1 (or $2N+2$) would be multiplied by a suitable constant—say, M. This would modify the input (or output) impedance of the filter by the factor M^2.

The congruence transformation and the transformation of Fig. 16 may be carried out in any sequence or may be intermixed. Both transformations are particularly useful when programmed for an interactive time-share computer terminal.

IV. Summary and Conclusions

Approximate theory and design equations for hairpin-line and hybrid hairpin-line/half-wave parallel-coupled-line filters have been presented. The theory and equations are based on the assumption that inductive coupling beyond the nearest neighbors is negligible. Although more difficult to satisfy than the usual and dual assumption of negligible capacitive coupling beyond the nearest neighbors, the former assumption leads to relatively simple equivalent circuits and design procedures. On the other hand, the latter assumption leads to quite complicated equivalent circuits that preclude any likelihood of achieving practical design procedures. The approximate design procedure is a set of self-consistant rules that permits the engineer to design hairpin-line, hybrid hairpin-line/half-wave parallel-coupled-line, or half-wave parallel-coupled line filters in a systematic and simple way.

Analysis of several theoretical designs using an "exact" equivalent circuit showed that the approximate theory yields nearly equiripple designs (in Chebyshev cases), but over a diminished bandwidth from the nominal value. The bandwidth contraction, however, can be compensated for by using a universal bandwidth contraction curve presented in the paper. Consequently, the approximate design equations are judged to be satisfactory for bandwidths of very narrow to approximately 25 percent. Interestingly, this is near the practical limit for realizing these filters with coplanar coupled lines.

A number of trial stripline and MIC filters of 5- and 20-percent bandwidths were constructed and tested. The experimental data for hairpin-line and hybrid filters *constructed in stripline* were judged to be in relatively good agreement with the approximate theory after the bandwidth contraction factor was accounted for. However, there was additional bandwidth contraction perhaps due to the finite line lengths connecting line pairs constituting hairpin resonators.

The experimental data for stripline filters also revealed the presence of a surface-wave mode that tended to give spurious passbands at Nf_0, where N is an even integer and f_0 is the center frequency of the filter. However, it was demonstrated that these spurious responses can be substantially reduced by two methods: 1) by using a hybrid geometry that interrupts the path of the surface-wave mode between input and output ports, and/or 2) by using a dielectric filler to eliminate the air gaps at the dielectric interface, thereby reducing the coupling to the surface-wave mode.

The experimental data for hairpin-line filters *constructed in* MIC compared moderately well in the passband with the approximate theory after allowing for bandwidth contraction. However, the stopband performances were severely degraded because of the presence of a surface-wave mode that propagated at frequencies just above the principal passband of the filters. Specifically, it was found that the surface-wave mode had a cutoff frequency corresponding to when the hairpin resonators are approximately a wavelength in the dielectric. The surface-wave mode was always excited in MIC filters. To date, the only practical way of overcoming the effect of the surface-wave mode is to utilize a hybrid geometry such that the surface-wave path between the input and output is interrupted. With this method, hybrid hairpin-line/half-wave parallel-coupled-line filters may prove satisfactory in MIC media, while still allowing a considerable degree of flexibility to the design engineer.

Acknowledgment

The authors wish to thank E. Fernandes, who carefully and skillfully fabricated all of the experimental filters described in this paper and recorded many of the experimental data.

References

[1] J. T. Bolljahn and G. L. Matthaei, "A study of the phase and filter properties of arrays of parallel conductors between ground planes," *Proc. IRE*, vol. 50, pp. 299–311, Mar. 1962.
[2] S. Frankel, "Equivalent circuits for TEM structures with periodic terminations," in *Proc. 1971 IEEE Region 6 Conf.* (Sacramento, Calif., May 11–13), Paper 5B-3, 1971.
[3] R. Sato and E. G. Cristal, "Simplified analysis of coupled transmission-line networks," *IEEE Trans. Microwave Theory Tech.*, vol. MTT-18, pp. 122–131, Mar. 1970.
[4] A. Podell, "A high directivity microstrip coupler technique," in *IEEE G-MTT 1970 Int. Symp. Dig.* (May 11–14), pp. 33–36, 1970.
[5] E. G. Cristal, "New design equations for a class of microwave filters," *IEEE Trans. Microwave Theory Tech.* (Corresp.), vol. MTT-19, pp. 486–490, May 1971.
[6] G. L. Matthaei, L. Young, and E. M. T. Jones, *Design of Microwave Filters, Impedance-Matching Networks, and Coupling Structures*. New York: McGraw-Hill, 1964.
[7] L. Weinberg, *Network Analysis and Synthesis*. New York: McGraw-Hill, 1962.
[8] R. J. Wenzel and M. C. Horton, "Exact design techniques for microwave filters," Bendix Research Lab., Southfield, Mich., Final Rep., Contract DA28-043-AMC-00399(E), Feb. 1–Apr. 30, 1965.
[9] G. L. Matthaei, "Interdigital band-pass filters," *IEEE Trans. Microwave Theory Tech.* (*1962 Symposium Issue*), vol. MTT-10, pp. 479–491, Nov. 1962.
[10] R. J. Wenzel, "Theoretical and practical applications of capacitance matrix transformations to TEM network design," *IEEE Trans. Microwave Theory Tech.* (*1966 Symposium Issue*), vol. MTT-14, pp. 635–647, Dec. 1966.